Solar diurnal anisotropy measured using muons in GRAPES-3 experiment in 2006

P K MOHANTY[1], D ATRI[1], S R DUGAD[1], S K GUPTA[1,*],
B HARIHARAN[1], Y HAYASHI[2], A JAIN[1], S KAWAKAMI[2],
S D MORRIS[1], P K NAYAK[1], A OSHIMA[2] and B S RAO[1]

[1]HECR Group, Tata Institute of Fundamental Research, Homi Bhabha Road, Mumbai 400 005,
India and GRAPES-3 Experiment, Cosmic Ray Laboratory, Ooty 643 001, India
[2]Graduate School of Science, Osaka City University, Osaka 558-8585, Japan
*Corresponding author. E-mail: gupta@grapes.tifr.res.in

Abstract. The GRAPES-3 experiment at Ooty contains a large-area (560 m^2) tracking muon detector. This detector consists of 16 modules, each 35 m^2 in area, that are grouped into four supermodules of 140 m^2 each. The threshold energy of muons is $\sec(\theta)$ GeV along a direction with zenith angle θ and the angular resolution of the muon detector is 6°. Typically, it records $\sim$4×10^9 muons every day. The muon detector has been operating uninterruptedly since 2001, thus providing a high statistics record of the cosmic ray flux as a function of time over one decade. However, prior to using these data, the muon rate has to be corrected for two important atmospheric effects, namely, variations in atmospheric pressure and temperature. Because of the near equatorial location of Ooty (11.4°N), the seasonal variations in the atmospheric temperature are relatively small and shall be ignored here. Due to proximity to the equator, the pressure changes at Ooty display a dominant 12 h periodic behaviour in addition to other seasonal changes. Here, we discuss various aspects of a novel method for accurate pressure measurement and subsequent corrections applied to the GRAPES-3 muon data to correct these pressure-induced variations. The pressure-corrected muon data are used to measure the profile of the solar diurnal anisotropy during 2006. The data, when divided into four segments, display significant variation both in the amplitude ($\sim$45%) and phase ($\sim$42 m) of the solar diurnal anisotropy during 2006, which was a period of relatively low solar activity.

Keywords. Cosmic rays; muons; muon detector.

PACS Nos 98.70.Sa; 14.60.Ef; 95.55.Vj

1. Introduction

Primary cosmic rays impinging the atmosphere interact in its upper layers through a sequence of interactions with the nuclei present in air. These interactions create secondaries that propagate further downwards creating still more secondary particles [1]. These

secondary particles contain mesons including pions and a smaller number of kaons. The decay of charged pions and kaons results in the production of muons. The muons, due to a relatively long lifetime and an energy loss mechanism caused only by ionization, survive deep down into the atmosphere. In fact, muons constitute the most abundant component of the secondary cosmic rays at sea level and higher energy muons can even penetrate deep underground. Most of the muons are produced higher up in the atmosphere at altitudes of several kilometres and suffer an energy loss of $\lesssim 2$ GeV due to ionization prior to reaching the sea level. The muon energy spectrum and angular distribution may be derived by folding their production spectrum with the energy losses in atmosphere, and by accounting for decays. The mean energy of muons at sea level is ~ 4 GeV with a relatively flat energy spectrum up to 1 GeV that gradually steepens thereafter. The integral flux of muons above 1 GeV at sea level is ~ 70 m^{-2} s^{-1} sr^{-1} and increases only slowly at higher altitudes. The angular distribution of muons arriving along a zenith direction θ varies as $\cos^2(\theta)$ for ~ 1 GeV energies [2,3].

As the flux of primary cosmic rays is nearly constant, the resultant secondary flux of the particles, including that of muons, should also be independent of time. Bulk of the muons detected at ground level is produced by relatively lower-energy (<100 GeV) primary cosmic rays that are modulated by solar energetic particles and associated magnetic field. Therefore, the muon flux also undergoes modulation by these solar effects and thus displays a 24-h periodicity due to the rotation of the Earth. However, at low Earth latitudes, the measurements of muon flux at ground level including the data from the GRAPES-3 experiment [4] show a dominant 12-h periodicity in addition to a weaker 24-h periodicity. A 12-h periodicity in the atmospheric pressure is caused by thermal heating of the upper atmosphere by the Sun. This heating results in a 12 h oscillation in the atmospheric pressure, that has been termed 'atmospheric tides' with an amplitude of ~ 1 mb near the equator, and it rapidly decreases at higher latitudes. This in turn results in a corresponding variation in the muon flux with the same 12 h period. In this context, it is interesting to recall that the phenomenon of atmospheric tides due to celestial and thermal effects was expected and actively studied since the days of Newton and Laplace. Yet it took over two centuries for a reasonably comprehensive understanding of this delicate and complex phenomenon to emerge [5].

Variability in the flux of primary cosmic rays has been studied for over seven decades. The initial measurements established the central role of the Sun in driving the cosmic ray variations [6]. Subsequent studies have employed a variety of instruments including scintillators, proportional counters, Cherenkov detectors and their various combinations. However, the primary objectives of these studies were to probe the variation of cosmic rays using either the secondary neutrons [7] or muons [8]. Both of these secondary components offer complementary information on cosmic ray variation. Unfortunately, the variation in atmospheric properties further complicates the interpretation of the results obtained from neutron monitors or muon detectors. Therefore, before proceeding with the analysis of the data, it is imperative to understand the impact of atmospheric parameters on the measured rates.

Neutron monitors, in general, probe the variation of cosmic rays at relatively lower energies of a few GeV. On the other hand, the muon detectors are sensitive to variations at higher energies ($\gtrsim 10$ GeV). At energies up to 100 GeV, the primary driver for most variations are a variety of Sun-induced phenomena, including the solar flares, coronal

mass ejections, coronal holes, Sun spot activities, solar rotation and shocks propagating in the interplanetary medium caused by various solar activities. However, before any studies of these variations are made, it is necessary to make corrections for local effects such as the changes in atmospheric properties, detector efficiencies etc. Prior to analysing the neutron monitor data, it is essential to correct for the effects of changes in atmospheric pressure [7].

Typically, a muon detector consists of several layers of charged particle detectors (proportional counters, scintillators etc.) that are separated by intervening layers of the absorber such as concrete or metal. In many instances, a muon detector is constructed as a rigid immovable structure. Thus, the threshold energy for muon detection increases with the arrival angle. The use of multilayer detectors with good position resolution allows the direction of incident muons to be determined to a precision of $\gtrsim 1°$. For example, in the case of GRAPES-3 experiment, the muon detector was constructed in the form of a rigid structure and therefore, its threshold energy varies as $\sec(\theta)$ GeV for an arrival direction with zenith angle θ. The use of four orthogonal layers of proportional counters permits measurement of the muon direction from a fairly large solid angle ($\sim$3 sr). This tracking capability allows the selection of muons from a given direction in the celestial hemisphere for studying cosmic ray variations. A total area of 560 m^2 of the GRAPES-3 muon detector results in a large rate of 4×10^9 d^{-1} of >1 GeV muons [4]. This large rate of muons offers a very sensitive probe for studying the variations in primary cosmic rays due to a variety of atmospheric and solar phenomena.

The analysis of the muon data is far more complex because corrections for changes in the atmosphere for both pressure- and temperature-induced effects have to be taken into account [8]. This is primarily because the muons are produced in the upper layers of the atmosphere through decay of mesons. A change in local temperature modifies the atmospheric density, and that in turn affects the balance between the two competing processes of decay and hadronic interactions of these mesons. For example, an increase in the temperature of the upper atmosphere can effectively reduce its local density due to expansion thereby increasing the probability of meson decay relative to interaction, resulting in a net increase in the muon flux. However, a less dense atmosphere increases the probability of muon decay thereby decreasing their flux. Thus, these two competing processes of decays of mesons and muons work against each other resulting in temperature coefficients that are positive and negative, respectively. The net outcome of this competition is a fairly complex process that can be calculated provided the density and temperature profiles of the atmosphere at the observing site are known. In the past, many calculations have been performed to estimate the effect of atmospheric temperature on the muon flux [9]. In a more recent work by a Russian group, details of the hadronic interactions and atmospheric profile were taken into account to provide extensive calculations of differential temperature coefficients for the muon flux that seem to agree well with the observed data [10].

Unlike the GRAPES-3 experiment, underground experiments such as MACRO [11], MINOS [12], and ICE-CUBE [13] detect muons of much higher energy (hundreds of GeV). These muons are produced higher up in the atmosphere due to decays of mesons of much higher energies. Therefore, the variation in the flux of these muons is subjected to the changes in the temperature of the upper atmosphere. For the ICE-CUBE experiment, the seasonal variation in the temperature over an year is rather large due to its polar location

[13]. However, the atmosphere above the GRAPES-3 experiment, due its near equatorial location (11.4°N), experiences temperature variations that are relatively small. The low-energy muons detected in GRAPES-3 are produced over the full height of the atmosphere. The effects of changes in the temperature profile of the atmosphere on the muon flux are further reduced due to this averaging process in the height of production of muons in the atmosphere. In the subsequent analysis of the GRAPES-3 data we have ignored the seasonal variations in the flux of muons due to changes in atmospheric temperature. Hereafter, the corrections are made only for the changes in the atmospheric pressure.

The cosmic rays reaching the Earth are modulated by solar effects and the solar diurnal anisotropy is one of the sources of this modulation. Traditionally, it has been difficult to measure the solar diurnal anisotropy because of its small amplitude. A precise determination of the long-term and day-to-day characteristics of this anisotropy is of prime importance for developing theoretical models of the processes whereby the Sun exercises control over the electromagnetic conditions in the inner solar system [14]. The solar diurnal variation in galactic cosmic rays at high rigidities can be used to obtain information on the parallel mean free path and the radial density gradient of cosmic rays [15].

In §2 the method used to calibrate the two digital barometers used in the GRAPES-3 experiment for pressure correction is described. The pressure correction parameter is determined by using a novel technique to identify the weekly GRAPES-3 muon data segments that are least influenced by the solar activity as described in §3. The pressure-corrected muon rate is used to measure the solar diurnal anisotropy during 2006 as detailed in §4. A summary of this study is presented in §5.

2. The pressure calibration

The GRAPES-3 experiment is located at Ooty (11.4°N, 76.7°E and 2200 m altitude) in India. It consists of an air shower array with a compact configurations of 1 m² plastic scintillator detectors with a separation of 8 m between adjacent detectors deployed in a symmetric hexagonal geometry. The observations were started in 2001 with 217 detectors that were subsequently expanded to about 400 detectors [16]. A very large tracking muon detector is also in operation as a part of this experiment. The muon detector is capable of measuring the directional flux of muons with high statistical accuracy. The muon detector has a total area of 560 m², consisting of 16 modules, each 35 m² in area. These modules are located close to each other as a cluster of four 35 m² neighbouring modules under a common roof termed as supermodule. Four supermodules with a total area of 4×140 m² $= 560$ m² constitute the GRAPES-3 tracking muon detector. The threshold energy of the muon detector is $\sec(\theta)$ GeV for muons arriving along a zenith direction θ [4].

As mentioned in §1, the observed rate of muons changes with atmospheric pressure and temperature. However, as explained in §1, here we have ignored the effects of changes in atmospheric temperature on the muons rate. Thus, a careful measurement of atmospheric pressure has become a key requirement for this experiment. This objective has been achieved by using two independent digital barometers and by a careful study of their long-term performance over a period of one year during 2006 as detailed below. The first barometer was a weather station manufactured by Davis Instruments, hereafter called WS [17]. It measured a number of weather parameters including the temperature,

humidity, rain fall, wind speed, wind direction etc. besides the atmospheric pressure. The second barometer PTB200 [18] located inside a muon supermodule, hereafter called BR, measured only the atmospheric pressure. The WS containing a controller along with the pressure and temperature sensors was located inside the control room. A second temperature sensor, along with rain and wind gauges, was placed outside the building. Thus the temperatures T_{in} inside and T_{out} outside the control room were provided by the WS. Both WS and BR logged data once every minute. The least count in the pressure measurement for both instruments was 0.1 hecto-pascal (hPa). The WS and BR data are automatically transferred to a data recording computer, once in a day.

For a successful correction of muon rate due to variation in pressure, it is essential to have an uninterrupted measurement of pressure for the entire duration of data. However, in practice gaps had occurred in the pressure data collected both by the WS and BR due to problems in the computer recording the data or due to unexpected power failures. For example, during the year 2006, there were no data for 0.43% of time from WS and 3.3% of time from BR. However, as both of these instruments recorded data on different PCs and were operated on independent power supplies, the probability of both of them failing simultaneously became highly unlikely. This feature was exploited to generate an uninterrupted series of pressure measurements provided the two instruments could be calibrated in a self-consistent manner. A comparison of the pressure measured by the two instruments from 1 to 8 January 2006 is shown in figure 1.

The upper plot in figure 1 shows the WS data and the lower plot shows the BR data. An oscillation with a period of 12 h in pressure is clearly visible in both datasets. This is in addition to the systematic difference in the pressure measured by these two instruments. The peak-to-peak amplitude of the 12 h variation is about 2.5 hPa. The mean pressure from WS data for this period is 788.5 hPa that translates into a fractional peak-to-peak amplitude of 0.32%. As the pressure measured by WS is systematically higher than BR, it
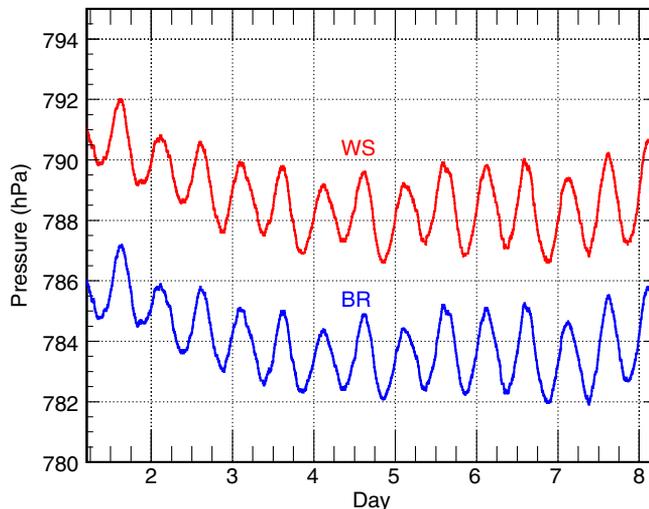

Figure 1. Pressure data. The upper plot shows the WS data and the lower plot shows the BR data.
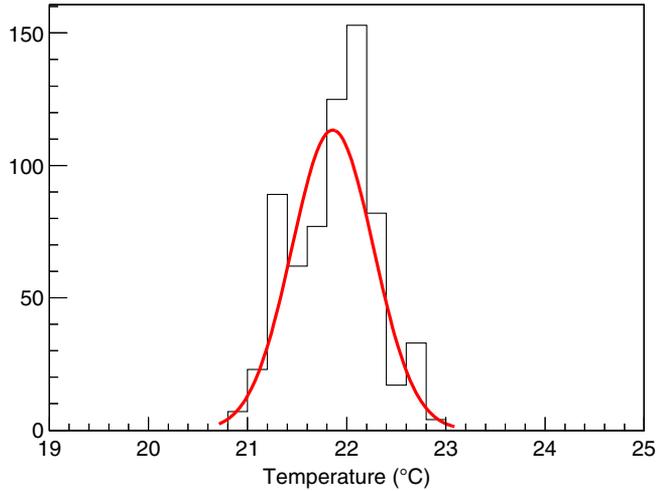
was initially suspected to be due to a difference in the calibration of these two instruments. However, a careful examination of the pressure difference showed that it was also due to the temperature of the WS, located inside the control room. To study this systematic behaviour, the fractional difference in pressure measured by the two instruments given by $\Delta P/P_{BR}$ was calculated, where $\Delta P = P_{WS} - P_{BR}$. The value of $\Delta P/P_{BR}$ as a function of time over a period of seven days from 1 to 8 January 2006 is shown in figure 2a. The variation of temperature T measured in the control room, where WS was kept, is also shown in figure 2b for comparison.

A clear-cut anticorrelation between the two parameters, $\Delta P/P_{BR}$ and the control room temperature T, is visible. As shown in figure 2b, the variation in temperature inside the control room is nearly $10°$ which influences the fractional calibration of WS by about 0.08%. It implies a variation of 0.01% in $\Delta P/P_{BR}$ for every $1°C$ change in temperature. As BR is kept inside one of the muon supermodules under an overburden of 600 g cm^{-2}, the variation in its temperature was very small. The distribution of the mean temperature taken every 15 min for the period of 1–8 January 2006 is shown in figure 3. A Gaussian fit to the data yields a standard deviation of only $0.4°C$. This results in a rather tiny change in the calibration of BR over time and we may attribute the observed variation in the magnitude of $\Delta P/P_{BR}$ entirely to the changes in the calibration of WS due to variation in temperature inside the control room.

The anticorrelation between the parameters $\Delta P/P_{BR}$ and the control room temperature T was further studied by analysing the data for the entire year. The values of parameters $\Delta P/P_{BR}$ and T were determined for successive intervals of 15 min. The data for a given value of T were grouped and the mean of the distribution of $\Delta P/P_{BR}$ labelled $\langle\Delta P\rangle/P_{BR}$ was obtained. A plot of $\langle\Delta P\rangle/P_{BR}$ as a function of temperature T is shown in figure 4. Also shown in the same plot is the root mean square (rms) width of $\Delta P/P_{BR}$ at each temperature. However, in almost all instances the rms is smaller than the size of the symbol used and hence remains invisible. This established the strong anticorrelation

Figure 2. Variation of (**a**) fractional pressure $\Delta P/P_{BR}$ and (**b**) temperature T in the control room over a period of one week.

Figure 3. Temperature distribution inside the muon supermodule. Gaussian fit yields $\sigma = 0.4°C$.

between $\langle \Delta P \rangle / P_{BR}$ and T. The magnitude of this anticorrelation is well described by the linear relation $\Delta P / P_{BR} = a + bT$, where a and b are the intercept and the slope, respectively of straight line fit to the data shown in figure 4. This yields a slope of $(-0.0097 \pm 0.0002)\%$ per °C for the pressure measured by WS. Therefore, a change of 10°C in temperature on a typical day causes an error of 0.1% in the pressure measured by WS. Although, numerically this appears to be a tiny effect, it is equivalent to $\sim 30\%$ of the change in pressure caused by atmospheric tides described in §1 and therefore, this effect has to be corrected appropriately.
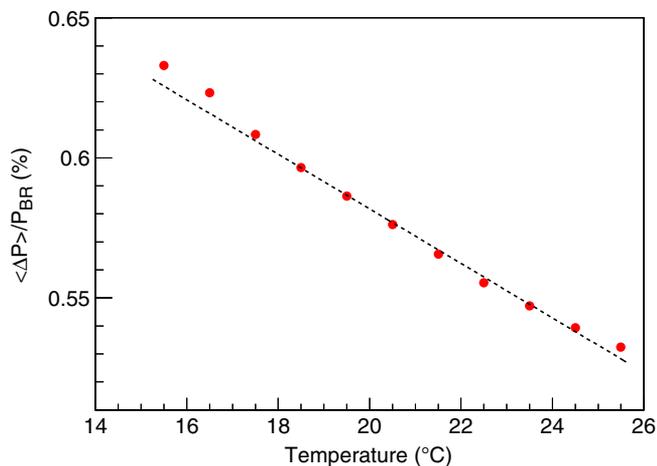
Figure 4. Variation of fractional pressure difference $\Delta P / P_{BR}$ with temperature T in the control room.
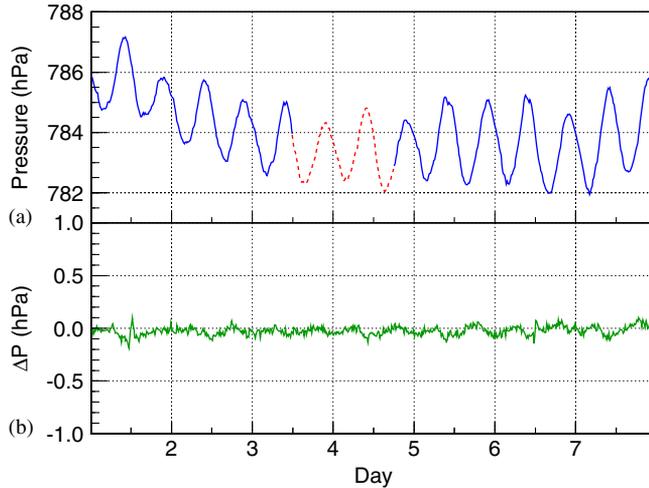
Figure 5. (**a**) Variation of pressure with time. Continuous line indicates BR and dotted line indicates WS after correction, (**b**) ΔP in hPa.

In figure 5a, the pressure measured by BR is shown by a continuous line. Also shown in figure 5a is the temperature-corrected pressure derived from WS for a short period shown by a dotted line. The smooth merger of the two sets of values testifies to the effectiveness of this conversion technique. The difference in the pressure measured by BR and WS is shown in figure 5b, that is centred on zero with a very small root mean square deviation of only 0.04 hPa.

The close agreement between pressure values from these two instruments enabled us to successfully complete two important tasks. As the BR is in an environment with very low temperature variation, the WS could be accurately calibrated for temperature dependence and corrected. This enabled us to constantly monitor the pressure using two stable devices with complete redundancy. Second, in the case of a failure of any one of these two devices, we could use the other one to obtain uninterrupted information on pressure. This was essential to obtain an unbroken record of cosmic ray muon flux by applying an appropriate correction for pressure variation as detailed in the next section.

3. The pressure correction

The variation in the atmospheric pressure shows an unambiguous 12 h periodic behaviour as seen from figure 5a which is caused by atmospheric tides as described in §1. Although the amplitude of this variation is rather small ($\sim$1 hPa), it produces a significant change in the observed muon rate that can be precisely measured in the GRAPES-3 data. The phase of the pressure minimum occurs at around 4 AM and 4 PM Indian Standard Time and the maximum occurs six hours later at 10 AM and 10 PM, respectively as seen from figure 5a.

The mean muon rate of 16 modules measured every 15 min for one week interval from 26 February to 4 March 2006 is shown in figure 6a and the value of pressure corresponding to the same time interval is shown in figure 6b. A clear anticorrelation between the muon rate and atmospheric pressure may be seen along with a dominant 12-h periodicity in
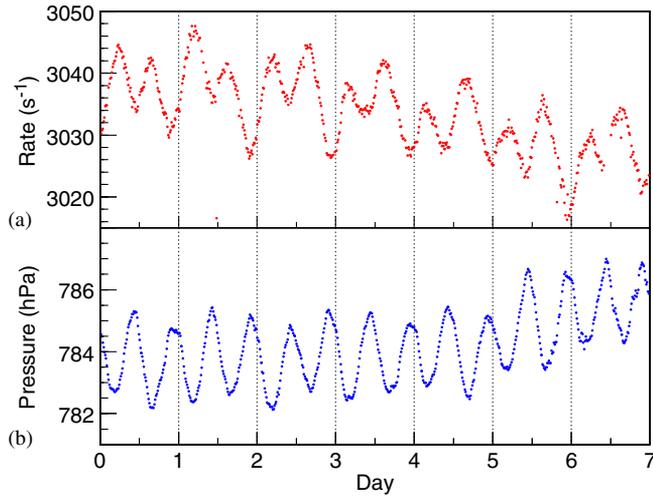
Figure 6. Variation of (**a**) mean muon rate and (**b**) pressure (hPa) for the week 26 February–4 March 2006.

both datasets as described in §1. One of the objectives of the present work described here is to measure this pressure dependence of the muon rate and correct this atmospheric effect prior to further analysis of the data for obtaining the solar diurnal anisotropy. A careful examination of the plots in figures 6a and 6b shows that while the pressure data display an almost sinusoidal profile riding on a slowly rising ambient pressure, the muon rate data exhibit a far more complex profile. This complexity primarily arises due to the presence of solar diurnal anisotropy that modulates the muon rate with a 24 h period and the interference of these two periodicities (12 and 24 h) results in the observed muon rate profile. If the effects of changes in the atmospheric pressure are taken into account, then one should be able to extract the solar diurnal anisotropy from the GRAPES-3 muon data.

The entire dataset from 2006 was divided into successive intervals (35040) of 15 min duration. Next, only those intervals when all 16 muon detector modules were working were selected. With this cut the data from a total of 37 weeks consisting of 21451 intervals were identified for further analysis. The mean muon rate of 16 modules as a function of atmospheric pressure is shown in figure 7. The error bar on each data point refers to the spread in the measurement of muon rate as obtained from the data itself. Clearly, the dependence of the muon rate on pressure is complicated by the interference of solar diurnal anisotropy. A linear fit to the data shown in figure 7 gives a rather poor fit with a large value of $\chi^2 = 25.1$ per degree of freedom (dof).

In order to isolate the effects of various external phenomena, the data were divided into weekly intervals and plots similar to the one shown in figure 7 were generated for each week and the χ^2 per degree of freedom for a linear fit to the data was obtained. Ideally, each week should contain 672 15-min samples. However, in reality, due to the dead-time in the data acquisition system and the breaks in data taking due to various problems, this number will be smaller than the limit of 672. A cut of 500 on the minimum number of 15-min samples and a requirement on the normalized $\chi^2 \leq 3.0$ was imposed for the selection of data from a given week for further analysis.
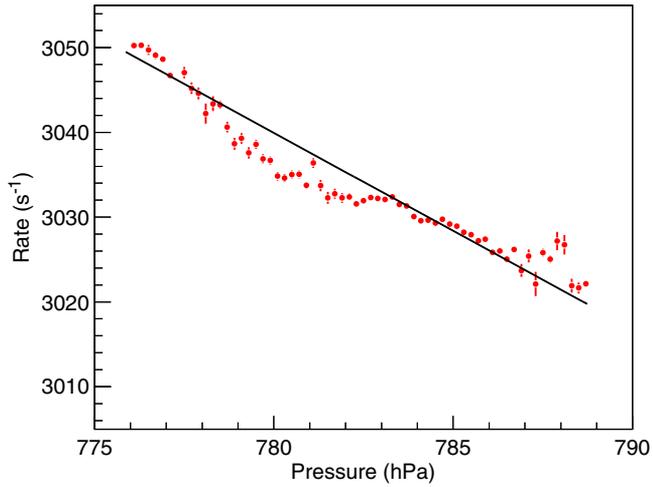
Figure 7. Variation of mean muon rate as a function of atmospheric pressure (hPa) during 37 weeks in 2006. Normalized $\chi^2 = 25.1$ per dof.
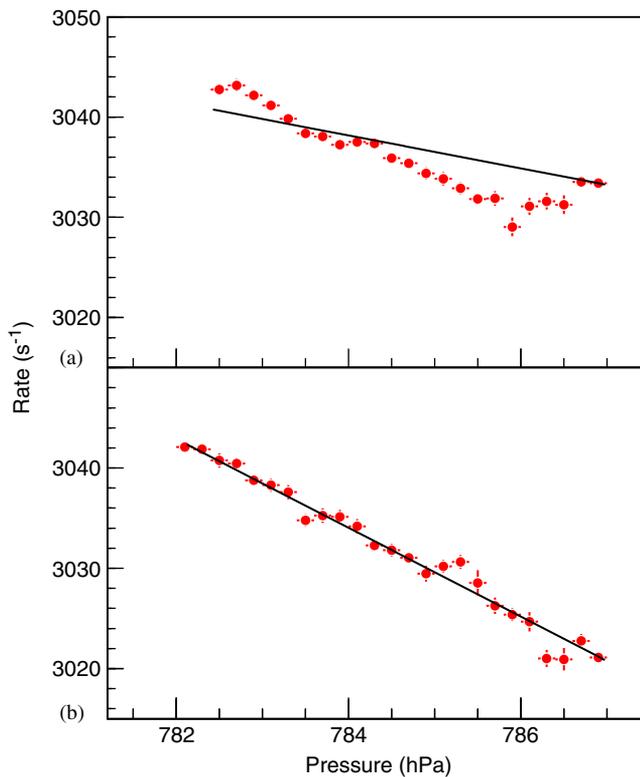

Figure 8. Variation of mean muon rate as a function of atmospheric pressure (hPa) for (**a**) week-7 $\chi^2 = 15$ and (**b**) week-9 $\chi^2 = 2.0$ per dof.
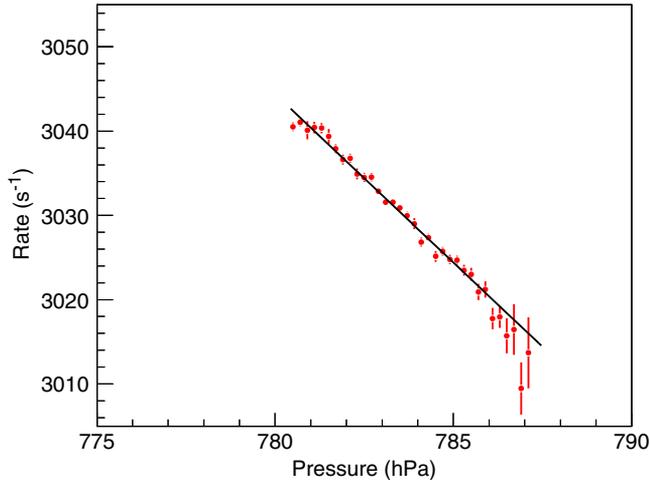
Figure 9. Variation of mean muon rate as a function of atmospheric pressure (hPa) for eight weeks selected with cuts, $\chi^2 \leq 3.0$ per dof, total 15-minute samples ≥ 500.

Data from a total of 8 out of 37 weeks passed these two stringent cuts. To appreciate the significance of the above cuts, the pressure dependence of the muon rate for weeks 7 and 9 are shown in figures 8a and 8b, respectively. The data from week 7 did not pass the cuts mentioned above, while week 9 did. From a comparison of the two plots in figure 8 it is clear that these cuts preferentially select the data that are less influenced by the solar diurnal anisotropy and consequently, their muon rate displays a linear dependence on the pressure. On the other hand, the data from week 7 yielded a rather poor fit.

The data of the eight weeks selected using the cuts described above were combined. The muon rate for the combined data as a function of pressure is shown in figure 9. The muon rate displays a clear linear dependence on pressure with a $\chi^2 = 2.4$ per dof. The percent change (R_c) in the muon rate as a function of pressure, derived from the linear fit shown in figure 9 is 0.132% per hPa. This value of R_c was used to correct the observed muon rate to a mean pressure of 784.1 hPa for the entire dataset spread over 37 weeks during 2006.

4. Solar diurnal anisotropy

The changes in atmospheric pressure and the solar diurnal anisotropy exhibit profiles with periods of 12 h and 24 h, respectively. These two effects are the principal causes of the observed variation in muon rate. The muon data collected over 37 weeks were folded modulo 24 h to examine these periodicities. The data folded prior to pressure correction display two peaks of unequal amplitude as shown in figure 10a. The same data after applying corrections for pressure variation as outlined in §3 are shown in figure 10b. After the correction, the variation due to the solar diurnal anisotropy becomes clearly visible in the folded data as seen in figure 10b.

The magnetic cut-off rigidity at Ooty is relatively large and varies from 14 GV in the west to 24 GV in the east with a value of 17 GV in the vertical direction [19,20]. Primary
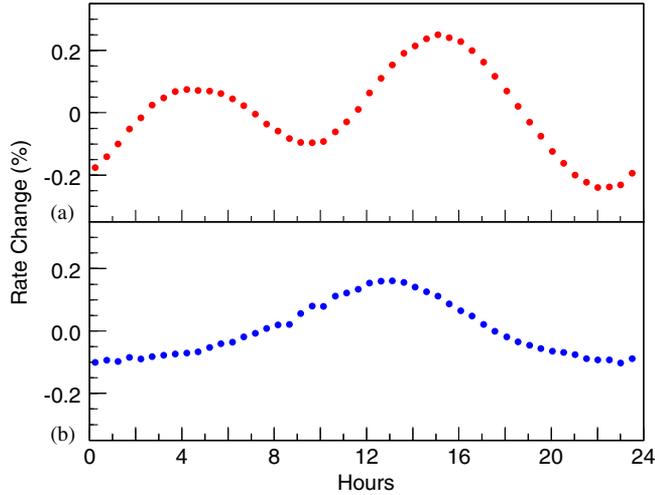
Figure 10. Mean muon rate folded modulo 24 h (**a**) before pressure correction and (**b**) after pressure correction.

cosmic rays entering the atmosphere above Ooty will have higher energy due to the high cut-off rigidity, and consequently the solar wind is expected to have a smaller impact on its flux. Therefore, the amplitude of solar diurnal anisotropy is expected to be rather small. The observed solar diurnal anisotropy averaged over the entire 2006, peaks with an amplitude of 0.26% at 12 h 57min Indian Standard Time (IST) with a mean amplitude of 0.11% as shown in figure 10b. The observed small amplitude of the solar diurnal anisotropy is entirely consistent with the high geomagnetic cut-off rigidity at Ooty. However, the high rate of muons detected by the GRAPES-3 allows effects as small as 0.01% to be measured.
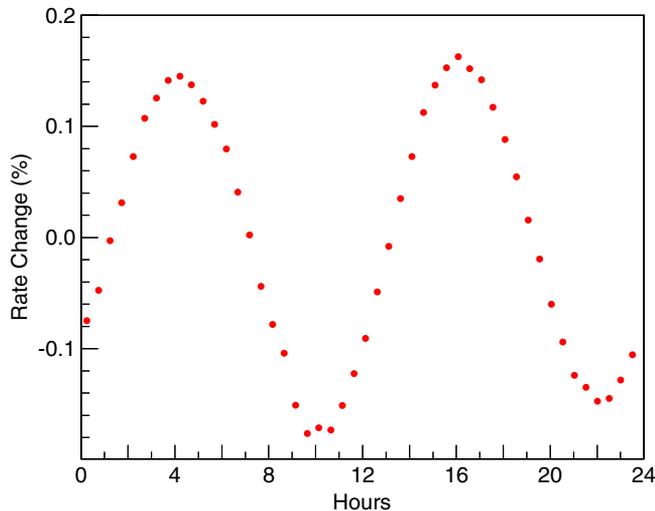
Figure 11. Pressure-induced correction to mean muon rate folded modulo 24 h.

The actual correction applied to the muon rate due to pressure variation was also folded modulo 24 h and the resultant plot is shown in figure 11. Not surprisingly, this plot displays a 12-h periodicity, that is equivalent to the difference in the plots shown in figures 10a and 10b. Next, we examined the variation in the profile of the solar diurnal anisotropy during 2006, by dividing the data into four segments of 9, 9, 10 and 9 weeks of actual observations. These segments correspond to an approximate period of 3 months each. Due to various problems and subsequent scheduled repair of affected detector modules, and the exacting requirement that all 16 modules be working simultaneously could only be met for 37 out of the 52 weeks in 2006 resulting in significant gaps in the data used here.
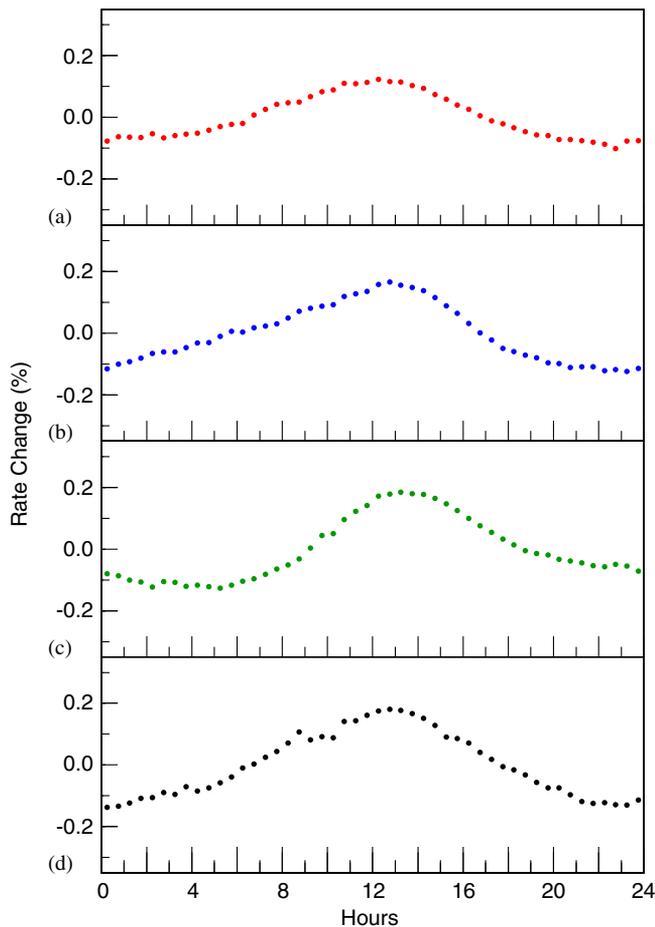
Figure 12. Solar diurnal anisotropy measured in 2006 from GRAPES-3 muon data for four segments. (**a**) 1 Jan.–4 Mar., peak at 12 h 20 min with an amplitude of 0.21%, (**b**) 5 Mar.–6 May, peak at 12 h 56 min with an amplitude of 0.28%, (**c**) 7 May–15 July, peak at 13 h 23 min with an amplitude of 0.31%, (**d**) 29 Oct.–30 Dec., peak at 13 h 02 min with an amplitude of 0.31%.

Table 1. Solar diurnal anisotropy parameters during the year 2006.

Interval	Pk Time	Pk Amp. (%)	⟨Amp.⟩ (%)	% Rise
1 Jan.–4 Mar.	12 h 20 min	0.212	0.107	0
5 Mar.–6 May	12 h 56 min	0.275	0.129	30
7 May–15 July	13 h 23 min	0.305	0.128	44
29 Oct.–30 Dec.	13 h 02 min	0.307	0.152	45

The solar diurnal anisotropy during the four segments of 2006 is shown in figure 12. The plot in figure 12a represents the anisotropy for the first segment from 1 January to 4 March 2006 that peaks with an amplitude of 0.21% at 12 h 20 min IST with a mean amplitude of 0.11%. The anisotropy for the second segment from 5 March to 6 May 2006 peaks with a 30% higher amplitude (relative to the first segment) of 0.28%, slightly later at 12 h 56 min IST with a mean amplitude of 0.13%. This trend continues during the third segment from 7 May to 15 July 2006 that peaks with a 44% (relative to the first segment) higher amplitude of 0.31% at 13 h 23 min IST with a mean amplitude of 0.13%. Finally, the fourth segment from 29 October to 30 December 2006 peaks with a 45% higher amplitude of 0.31% at 13 h 02 min IST with a mean amplitude of 0.15%. These quantitative parameters of the solar diurnal anisotropy measured from the GRAPES-3 data for 2006 are summarized in table 1. The correlation of these solar diurnal anisotropy measurements with various interplanetary parameters such as the magnetic field, plasma density, solar wind velocity etc. may provide a better understanding of the processes occurring in the inner solar system including the radial density gradient of cosmic rays.

5. Summary

The GRAPES-3 large-area (560 m^2) tracking muon detector consisting of 16 modules with a threshold energy of 1 GeV along the vertical direction is operating at Ooty since 2001. The muon detector records a huge number of ($\sim 4 \times 10^9$) muons every day and hence serves as a powerful tool for measuring tiny variations in the muon rate caused by atmospheric pressure, temperature and the solar activity. Due to the near equatorial location of Ooty (11.4°N), the seasonal variations in the atmospheric temperature are relatively small and hence were not considered here. However, before probing the influence of solar activity it became necessary to correct the measured muon rate for variation in atmospheric pressure. For this purpose, the data were divided into weekly segments and only those segments that had all 16 modules working were selected for further analysis and only 37 out of the 52 weeks met this stringent criterion. Next, the segments where muon detectors were working for at least 75% of the time ($\geq$500 out of 672 15-min interval in a week) and displaying very small solar activity were selected for determining the pressure correction of 0.132% per hPa.

After the pressure correction, the muon data when folded modulo 24 h showed a clearcut existence of the solar diurnal anisotropy with a peak amplitude of 0.26% at 12 h 57 min IST. The 2006 data were further divided into four segments to study the variation of

solar diurnal anisotropy over the whole year. The amplitude of the anisotropy gradually increased from 0.21% in the first segment to 0.31% in the third and fourth segments. The time of the peak amplitude of the anisotropy also displayed a gradual increase in delay, reaching a value of 63 min in the third segment relative to the first segment. Thereafter, this delay was reduced to 42 min in the fourth and final segment. These measurements are significant, since the Sun was in a relatively quiet phase during 2006 and therefore, the magnitude of the solar diurnal anisotropy was also relatively small. Yet the high sensitivity of the GRAPES-3 muon detector allowed a tiny amplitude (0.2–0.3%) of this anisotropy to be accurately measured and its shape determined. Future studies of the correlation of the solar diurnal anisotropy measurement with parameters of interplanetary space may help in understanding the space weather better.

Acknowledgements

References

 [1] K Greisen, *Ann. Rev. Nucl. Sci.* **10**, 63 (1960)
 [2] P K F Grieder, *Cosmic rays at Earth* (Elsevier Science, 2001)
 [3] K Nakamura *et al*, *J. Phys. G: Nucl. Part. Sci.* **37**, 075021 (2010)
 [4] Y Hayashi *et al*, *Nucl. Instrum. Methods A* **545**, 643 (2005)
 [5] R S Lindzen and S Chapman, *Space Sci. Rev.* **10**, 3 (1969)
 [6] S E Forbush, *Phys. Rev.* **54**, 975 (1938)
 [7] J A Simpson, *Space Sci. Rev.* **93**, 11 (2000)
 [8] M L Duldig, *Space Sci. Rev.* **93**, 207 (2000)
 [9] S Sagisaka, *Il Nuovo Cimento C* **9**, 809 (1986)
[10] A N Dmitrieva *et al*, *Astropart. Phys.* **34**, 401 (2011)
[11] M Ambrosio *et al*, *Astropart. Phys.* **7**, 109 (1997)
[12] P Adamson *et al*, *Phys. Rev. D* **81**, 012001 (2010)
[13] P Desiati *et al*, *Proc. 32nd Int. Cosmic Ray Conf.* (Beijing, 2011)
[14] S P Duggal *et al*, *Nature* **214**, 154 (1967)
[15] D L Hall *et al*, *Astrophys. J.* **482**, 1038 (1997)
[16] S K Gupta *et al*, *Nucl. Instrum. Methods A* **540**, 311 (2005)
[17] www.davis.com
[18] www.vaisala.com
[19] T Nonaka *et al*, *Phys. Rev. D* **74**, 052003 (2006)
[20] P Subramanian *et al*, *Astron. Astrophys.* **494**, 1107 (2009)